

Supplementary Material

High-accuracy measurement on heat of detonation with good robustness by laser induced breakdown spectroscopy of Energetic Materials

An Li,^a Xinyu Zhang,^a Yunsong Yin,^a Xianshuang Wang,^a Yage He,^a Yuheng Shan,^a Ying Zhang,^a Xiaodong Liu,^a Lixiang Zhong^{a*}, Ruibin Liu^{ab*}

^a *Key Lab of Precision Spectroscopy and Optoelectronic Technology, School of Physics, Beijing Institute of Technology, Beijing 100081, China.*

^b *Frontiers Science center for High Energy Material (MOE), Beijing Institute of Technology, Beijing 100081, China.*

*Corresponding author: Lixiang Zhong; Ruibin Liu

E-mail address: zhonglx@bit.edu.cn; liusir@bit.edu.cn

I. Detail of laser spot on the sample

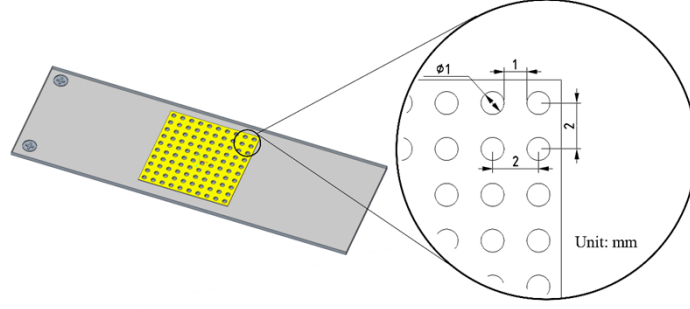


Fig.S1. The size of the laser ablation spot on the sample is about 1mm and the sampling distance is 2mm.

II. Physical model of the laser ablation process

In physical, the essence of the laser-matter interaction is initialized by coupling its electromagnetic field. The accelerated electrons collide with each other and transmit the energy to more electrons or lattices. Due to the lattice being heated, the thermal energy deposition is typically dominated when the nanosecond laser irradiates the matter, which is called the photothermal mechanism, and the material response can be treated in a purely thermal way¹. Consequently, the interaction between laser and matter is highly affected by the physical properties of materials once the laser parameters are determined². Thus, the process of laser ablation of materials can be described by the Fourier law as described in Eq. (1) ~ Eq. (4)³,

$$\rho C_p \frac{\partial T(x,y,t)}{\partial t} = \nabla \cdot [k \nabla T(x,y,t)] + I(y,t) \quad (1)$$

$$I(y,t) = I_s(t) \exp(-y) \quad (2)$$

$$I_t = I_{max} \exp \left[- \frac{\log(16)(t - \tau/2)^2}{FWHM^2} \right] \quad (3)$$

$$I_{max} = \frac{2F}{FWHM} \sqrt{\frac{\log(16)}{\pi}} \quad (4)$$

where C_p , ρ , k are specific heat, density, and thermal conductivity of the material, respectively. $I(y,t)$ is the term of laser heat representing the energy density of the laser applied to the material⁴, τ and F are the total pulse duration of laser and laser fluence, respectively. The thermal parameters of EMs are listed in Table. 1 in the main text. Note that the materials TKX50 and TNTNB are not simulated due to a lack of available thermal parameters.

The thermodynamic process of energetic materials under a nanosecond laser pulse is simulated by the simplified two-dimensional FEM (Finite Element Model), the energetic material is simulated as a rectangle with the size of $600 \mu\text{m} \times 50 \mu\text{m}$, when the laser irradiates the middle position (300, 50) of the model, the heat transfer to the Y depth and X direction respectively, as shown in Fig. S2(a), the top part of the figure marked the initial state of laser irradiates the material surface, and the bottom part of the figure marked an ablation crater formed after the laser interact on the material. FEM simulation assumes that absorption is mainly caused by the inverse bremsstrahlung while ignoring the plasma-laser interactions during laser irradiation because the laser interaction with EMs is accompanied by the exothermic chemical reaction, which involves many electrons consumed. It usually leads to lower electron density than non-energetic material during laser pulse irradiation, thus illustrating less

luminescence in laser-induced plasma implying a high detonation performance⁵. Moreover, a relatively low laser fluence of 1.2 GW/cm² is applied in the experiment, making it difficult to ionize excessive ions due to the high ionization potential of energetic material⁶. Therefore, most of the laser energy strikes energetic materials⁷. The volume of materials stripped from the material surface is found to be quite different for different EMs, the ablation volume of TNT is maximum, and the HNS has a minimum ablation volume, the material NTO, FOX7, and HMX has similar ablation volume, as illustrated in Fig. S2(b), indicating that the thermal interaction and ablation process are much different due to the different thermal properties of the various materials.

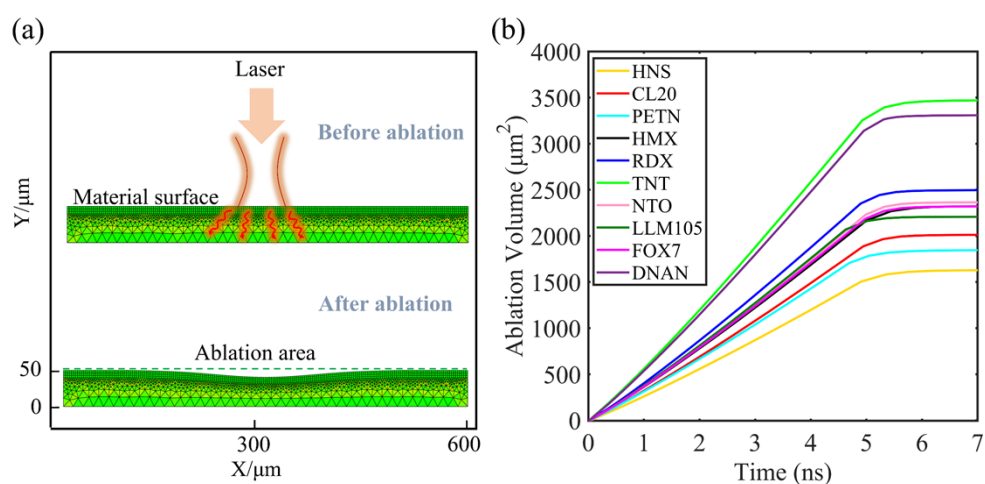


Fig. S2 The simulation of laser ablate EMs progress by FEM method (a) The schematic diagram of the physical model in 2-dimensional space (b) The time-variation of ablation volume during the laser pulse.

Physically, the stripped material transforms to plasma due to the enormous heat effect⁸. The plasma radiation characteristics should be different due to the formation of plasma originating from the various laser ablation volume of material⁹, that is, if thermal energy is confined in the local region with small thermal conductivity κ , the material would be heated rapidly in the micro-zone with the low specific heat C_p , and melting and vaporization occur instantaneously when the material has a low enthalpy of sublimation E_s , the plasma is easier to produce. These thermal progress simulation results provide a fundament for investigating the plasma spectral difference of various EMs. Based on the analysis above, we obtained laser induced plasma spectra of several energetic materials, and the quantitative analysis for the heat of detonation was implemented successfully.

To further clarify the associations between plasma emission features and laser ablation material volume in different EMs, we consider the whole spectral features instead of certain emissions. Thus, the spectra scores plot of ten EMs (CL-20, PETN, HMX, RDX, FOX-7, TNT, LLM105, NTO, HNS, DNAN) is calculated using the PCA method, which implied the relationship between spectral features, detonation heat of materials and the volume of material ablated by laser. As shown in Fig. S3(a), the scores of the first two PCs (principal components 1 and 2, explained 77% variance in total) discriminate the materials into two parts named D1 with the scores $t_1 < 0$ and D2 with the scores $t_1 > 0$ as marked by the red dashed circle in the figure, the white digits around the names are the values of the heat of detonation. The heat of detonation is 5.02 kJ/g~6.2 kJ/g of cluster D1, including five EMs, i.e., HMX, RDX, CL-20, FOX-7, and PETN. The cluster D2 comprises TNT, NTO, DANA, LLM105, and HNS, which have a slightly low heat of detonation within 3.5 kJ/g~4.4 kJ/g. Moreover, the scores of the second and third PC (principal components 2 and 3, explained 43% variance of data) divide ten EMs into three parts as marked by the blue dashed circle in Fig. S3(b), the domain A1 cluster five EMs together which have significantly

different heat of detonation but are close in laser ablation volume as shown by the white digits around the circle points in the figure. Similarly, the domain A2 cluster has three EMs, and A3 has two EMs enclosed. In addition, domain A1 has scores $t_2 > 0$ and scores $t_3 > 0$, domain A2 corresponds scores $t_2 < 0$ and scores $t_3 < 0$, and domain A3 is in the fourth quadrant with scores $t_2 > 0$ and scores $t_3 < 0$. The ellipse shadow is the Hotelling's T^2 (95%) region, and all the data points are located in the ellipse, indicating no outliers.

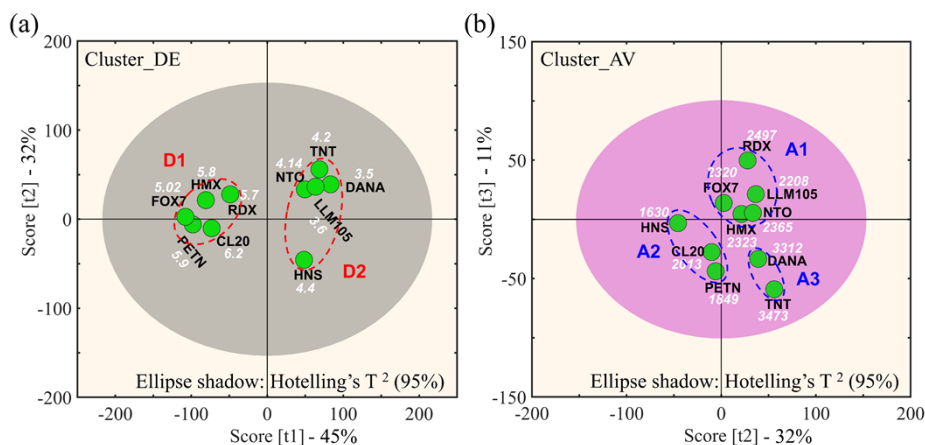


Fig. S3. The scores diagram of ten EMs spectral features in principal component space (a) The scores of the first two PCs divide materials with different heat of detonation (Cluster_DE) into two clusters (b) The scores of second and third PCs distribute the materials with different laser ablation volume (Cluster_AV) into three clusters.

Those scores of the first three PCs extract the latent spectral information related to the heat of detonation and the ablation volume according to Fig. S3, indicating the intensity of spectral emissions correlates with the detonation performance of EMs and the laser ablate EMs process. Once the initial ablation conditions are confirmed, the radiation intensity and the evolution pattern will be affected or even determined inside the plasma¹⁰.

Reference

1. D. Bauerle, M. v. Allmen and I. W. Boyd, *Laser-Beam Interactions with Materials: Physical Principles and Applications-Springer Berlin Heidelberg*, Springer, Berlin Heidelberg, 1987.
2. H. K. Malik, *Laser-Matter Interaction for Radiation and Energy* CRC Press, Boca Raton, 1st Edition edn., 2021.
3. J. Terragni and A. Miotello, *Micromachines (Basel)*, 2021, **12**.
4. Y. Lu, L. Yang, M. Wang and Y. Wang, *Appl Opt*, 2020, **59**, 7652-7659.
5. J. L. Gottfried, 2015, **30**, 674-681.
6. J. K. Cooper, C. D. Grant and J. Z. Zhang, *J Phys Chem A*, 2013, **117**, 6043-6051.
7. O. A. Ranjbar, Z. Lin and A. N. Volkov, *Applied Physics A*, 2020, **126**.
8. X. Li and Y. Guan, *Nanotechnology and Precision Engineering*, 2020, **3**, 105-125.
9. M. S. Brown and C. B. Arnold, *Fundamentals of Laser material interaction and application to multiscale surface modification*, Springer
10. J. Moros and J. Laserna, *Applied Spectroscopy*, 2019, **73**, 963-1011.